ACS APPLIED MATERIALS & INTERFACES

Research Article

www.acsami.org

Syndiotactic Polystyrene/Hybrid Silica Spheres of POSS Siloxane Composites Exhibiting Ultralow Dielectric Constant

Angel Mary Joseph,[†,‡] Baku Nagendra,[†,‡] K. P. Surendran,[*,†,‡] and E. Bhoje Gowd[*,†,‡]

[†]Materials Science and Technology Division (AcSIR), CSIR-National Institute for Interdisciplinary Science and Technology, Trivandrum 695019, Kerala, India

[‡]Academy of Scientific and Innovative Research (AcSIR), New Delhi 110 001, India

Supporting Information

ABSTRACT: Homogeneously dispersed hybrid silica/syndiotactic polystyrene composites were investigated for low-κ dielectric applications. The composites were prepared by a solution blending method, and their microstructures were analyzed by SEM, TEM, and AFM. Crystallization and phase transformation behavior of sPS were investigated using differential scanning calorimetry and wide-angle X-ray diffraction. These composites exhibited improved thermal stability and reduced thermal expansion coefficients. Promising dielectric properties were observed for the composites in the microwave frequency region with a dielectric constant (κ = 1.95) and loss (tan δ = 10^{-4}) at 5 GHz.

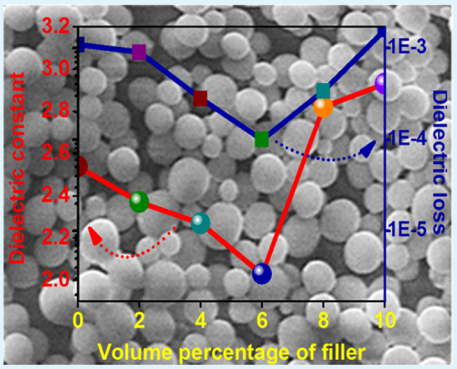

KEYWORDS: *syndiotactic polystyrene, hybrid silica, solution blending, thermal stability, crystallization, dielectric properties*

INTRODUCTION

The ever increasing demand for the portable and miniaturized electronic devices of the modern era exerts a constant thrust on the scientific community to develop novel low permittivity, low loss materials as an interlayer dielectric which can effectively reduce the resistance−capacitance (RC) delay and signal crosstalk and can prevent the leakage of current between the wiring elements in an integrated circuit (IC).[1−3] Mainly three methods are anticipated for the reduction of RC delay in the microprocessor, which includes adding more levels of wiring to decrease signal transit distances at the smallest wiring dimensions, replacing the aluminum wiring with copper, which is a metal of 30% lower resistivity, and, last, switching from silica (κ ∼ 3.9−4.2) to an insulator of lower dielectric constant.[4,5] Among these, the most feasible strategy is the development of alternate novel low-κ materials, which is equally interesting to the fundamental research as well as industry.

Low dielectric (low κ) materials are of crucial significance in the field of electronic packaging applications and substrate applications as well.[1,6,7] Although a plethora of organic, inorganic, and hybrid materials have been investigated for this purpose, most of them failed in the BEOL (backend of line) production.[4,8] In order to achieve low dielectric constants, two strategies were mainly adopted: either decrease the number of dipoles or decrease the dipole strength. Decreasing the number of dipoles in an ILD (interlayer dielectric) can be achieved by effectively reducing the density of the material, which is practically materialized by the introduction of additional porosity. Incorporation of air in the dense material will lead to decreased dielectric constant.[9] Polymers are promising materials for the realization of low-κ materials because of their inherently low dielectric constant, mostly below 3, and the hydrophobic properties that delimit water absorption. However, the principal challenge in their use is their low thermal robustness, particularly low softening temperature. For example, several aromatic polymers possess low dielectric constants, but their thermal and mechanical properties prevent them from being used as ILDs.[10] Against this background, polymer composites have been evolved as an effective alternative owing to their tunable dielectric, mechanical, and thermal properties with the prudent selection of fillers. Polyhedral oligomeric silsesquioxanes (POSS) and POSS siloxane hybrids have been widely studied as the effective fillers for the low dielectric polymer composites.[11,12] POSS exhibits an intrinsically low dielectric constant ∼ 2 due to its nanoporous (∼0.5 nm) cube cage structure.[13,14] Also, it exhibits the unique opportunity for preparing an organic inorganic hybrid material with an inorganic core containing Si−O−Si bonds and organic functional groups on the periphery that can increase the compatibility with the polymer matrix.[14] The incorporation of a POSS nanocluster cage into a polymeric material can result in dramatic improvements in the polymer's properties, including greater thermal and oxidation resistance, surface hardening, reduction in flammability, and improvements

Received: July 2, 2015
Accepted: August 19, 2015
Published: August 19, 2015

DOI: 10.1021/acsami.5b05933
ACS Appl. Mater. Interfaces 2015, 7, 19474−19483

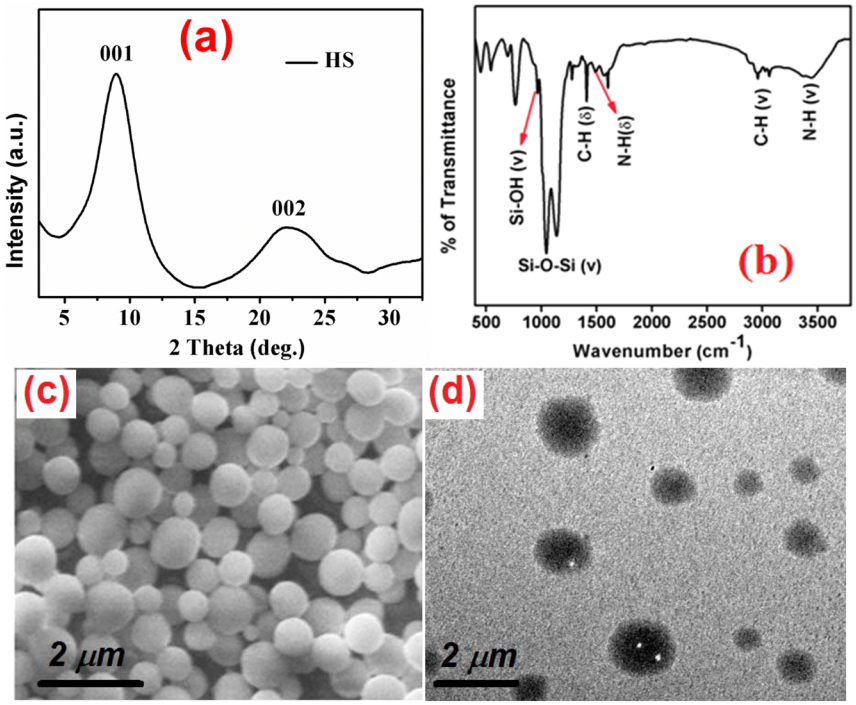

Figure 1. (a) WAXD pattern of HS. (b) FTIR pattern of HS spheres of POSS siloxane composition. (c) SEM and (d) TEM images of hybrid silica spheres of POSS siloxane composition.

in dielectric properties.[15] Sasikala et al. reported the synthesis of hybrid silica spheres (HS) of POSS siloxane composition that are compatible with hydrophobic polymers like polystyrene.[16]

It has been shown that the tacticity plays a significant role in determining the properties of polymeric materials. For example, the arrangement of the phenyl groups at alternate sides of the chain is supposed to lower the dielectric constant in syndiotactic polystyrene due to the reduced net polarization.[17] In this work, syndiotactic polystyrene (sPS) has been selected as the host matrix because of its high glass transition temperature, high melting point, fast crystallization rate, and good processing properties.[18,19] sPS is an interesting material that exhibits a high degree of polymorphism with five major crystalline forms (α, β, γ, δ, and ε) and some mesophases.[20,21] Among these crystalline forms, the β form is highly stable, and once formed, it will not undergo any transition in the presence of solvents or before melting (270 °C).

In the present investigation, composites of syndiotactic polystyrene and hybrid silica spheres have been prepared by the solution blending method, and the dielectric properties including the relative permittivity and dielectric loss were examined. The microwave dielectric constant was decreased to ultralow values of 1.95 (at 5 GHz) with a systematic addition of the filler with a promising low dielectric loss. Furthermore, the influence of hybrid silica spheres on the crystallization behavior and thermal stability of sPS was investigated.

EXPERIMENTAL SECTION

Materials. Triethoxyvinylsilane (97%), (3-aminopropyl)-triethoxysilane (99%), and xylene solvent were purchased from Aldrich Chemicals Co. Absolute ethanol has been received from Merck chemicals. Syndiotactic polystyrene (sPS) pellets (M_w: 272 000, M_w/M_n: 2.28) used in this study were kindly supplied by Idemitsu Petrochemical Co., Ltd. All the above chemicals and polymer were used as received. Millipore grade water was used for the synthesis of POSS.

Sample Preparation. Hybrid silica spheres of POSS−siloxane composition were synthesized using the method reported elsewhere.[22] Typically, vinyltriethoxysilane and aminopropyltriethoxysilane (3:1 molar ratio) were dissolved in a mixture of ethanol and water (15:1 V/V ratio). It was allowed to age for 7 days at ambient conditions. After aging, the solution was further diluted and the solvents were evaporated at ambient conditions. The composites of sPS with different volume percentages of HS were prepared by solution blending in xylene. The sPS granules were dissolved in xylene in a 100 mL round-bottom flask at a temperature of 170 °C. After the complete dissolution of sPS, the required amount of HS spheres was added to the solution under continuous stirring. The mixture was allowed to reflux at the same conditions for 7 h so that the homogeneous dispersion of the filler in the polymer matrix can be achieved. The resultant hot solution was reprecipitated with 100 mL of ethanol. The precipitate was filtered, washed with ethanol several times, and then dried in a vacuum oven at 120 °C. The samples for the dielectric measurements were prepared by hot-pressing techniques in a laminating press using suitable steel molds at a temperature of 200 °C and a pressure of 2 MPa for 90 min.

Characterization. The morphology of the samples including that of the pure hybrid silica and the sPS-HS composites were examined by scanning electron microscopy (Zeiss EVO 18 cryo SEM and JEOL-JSM 5600 LV). The as-prepared HS in the ethanol−water mixture was drop-casted onto the glass plate that was used for the SEM imaging. Thin films of sPS and sPS−HS composites were prepared by melt-pressing, and the surface morphology of these thin films was probed using SEM and AFM. For a more detailed viewing of the morphology of HS, transmission electron microscopy (TEM) analysis was also performed. TEM images were recorded using a JEOL 2010 transmission electron microscope. In order to understand the phase separation and morphological behavior of pristine polymer and the composites, atomic force microscopy (AFM) analysis in the tapping mode was carried out (Bruker Multimode, Germany). The average roughness and skewness of the surface were also estimated using AFM micrographs recorded at a scan size of 50 μm × 50 μm. The infrared spectra were recorded using a PerkinElmer Series FT-IR Spectrometer Two over the wavenumber range of 4000−400 cm^{-1}. For this purpose, the powder samples were mixed with KBr and pressed in the form of

DOI: 10.1021/acsami.5b05933
ACS Appl. Mater. Interfaces 2015, 7, 19474−19483

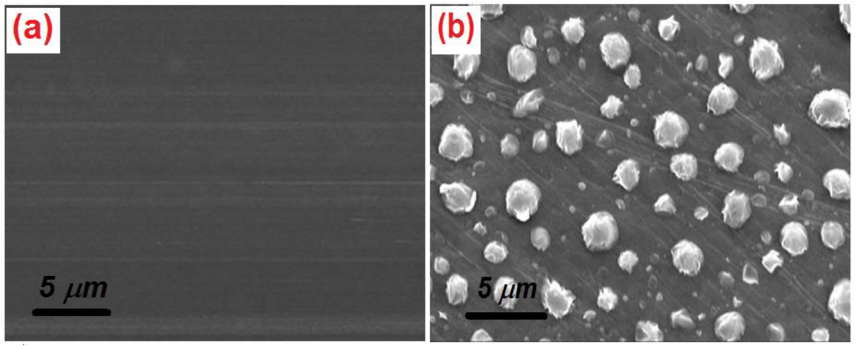

Figure 2. SEM images of (a) neat sPS film and (b) sPS−6 vol % HS composite.

pellets. The FTIR spectra were collected with 32 scans at a resolution of 1 cm^{-1}.

WAXD measurements were carried out to confirm the dispersion of the filler and to study the polymorphism of the host polymer with addition of the POSS moiety on a XEUSS SAXS/WAXS system using a Genix microsource from Xenocs operated at 50 kV and 0.6 mA. The Cu Kα radiation (λ = 1.54 Å) was collimated with a FOX2D mirror and two pairs of scatterless slits from Xenocs. The 2D patterns were recorded on a Mar345 image plate and processed using Fit2D software. All the measurements were made in the transmission mode. In order to figure out more details about the crystallization behavior, differential scanning calorimetric (DSC) analysis was conducted on a PerkinElmer Pyris 6 DSC. Here, the samples were heated from room temperature to 300 °C, which is above the melting temperature of sPS, at a rate of 10 °C/min. At 300 °C, it was held for 1 min to erase out all the thermal history of the sample, then cooled down to 250 °C at a rate of 50 °C/min, where it was kept for 30 min to facilitate isothermal crystallization. Again, the samples were heated to 300 °C at a rate of 10 °C/min and then cooled at a ramp rate of 10 °C/min to room temperature in order to measure the melt crystallization temperature (T_{mc}).

To understand the thermal stability, thermogravimetric analysis (TGA) was done using a thermogravimetric analyzer TA Q50 under nitrogen gas atmosphere at a heating rate of 10 °C/min. The coefficient of thermal expansion (CTE) was measured using a TMA analyzer (TMA/SS7300, SII NanoTechnology Inc.,Tokyo, Japan) in the temperature range of 30−150 °C by applying a pressure of 0.1 N. Moisture absorption by the composites was studied by measuring the weight gained by the samples (kept at 110 °C overnight) upon dipping in distilled water for 24 h, using a chemical balance with an accuracy of ±0.1 mg.

The dielectric properties of the samples in the radio frequency range from 300 Hz to 3 MHz were measured using an LCR meter (LCR HiTESTER, Hioki 3532-50) by the parallel plate capacitor method where both sides of the circular disc-shaped sample were coated with silver electrodes. The measurements were carried out at room temperature, and the dielectric data were derived from the complex impedance measurements. The dielectric properties in the microwave region (5 GHz) were calculated with a Split Post Dielectric Resonator (SPDR QWED, Poland) in the $TE_{01\delta}$ resonant mode with the aid of a vector network analyzer (Model No. E5071C ENA series; Agilent Technologies, Santa Clara, CA, USA). For this measurement, rectangular sample with dimensions of 40 mm × 40 mm × 1 mm was used.

RESULTS AND DISCUSSION

Hybrid silica spheres of POSS siloxane composition has been prepared by the hydrolytic co-condensation reaction of 3-aminopropyltriethoxysilane and vinyltriethoxysilane. The diffraction peaks at 2θ = 8° and 22° in the WAXS pattern (Figure 1a) belong to hybrid silica with POSS siloxane composition. It is already reported that the peak at 2θ ∼ 8° corresponds to the POSS cage, which arises due to some long-range order in POSS, and the one at 2θ ∼ 22° (corresponding to 002 plane) is attributed to the merged peak of the POSS bilayer assembly and the amorphous halo of incompletely condensed siloxane.[22,23] The relatively broader diffraction peak at 22° can be associated with Si−O−Si linkage.[24] The structure of hybrid silica spheres with POSS siloxane composition could be further established using the FTIR spectra given in Figure 1b, where the bands at 1050 and 1149 cm^{-1} are believed to be the characteristic peaks of the POSS moiety arising due to the symmetric stretching of Si−O−Si bonds and the symmetric stretching of Si−OH bonds.[25] The SEM and TEM images present the spherical morphology of the HS (see Figure 1c,d). It should be noted that the ratio between organic and inorganic components is crucial in maintaining the spherical morphology of hybrid particles during aging because of their different hydrophobic hydrophilic balance properties. From the electron microscopy analysis, the diameter of the prepared hybrid silica was found to be below 1 μm.

In principle, the SEM analysis can also be used as a tool to investigate the dispersion and compatibility of the filler in the polymer matrix and the extent of homogeneity in dispersion. The surface morphologies of the pristine polymer and its composite with 6 vol % hybrid silica are shown in Figure 2. From the SEM micrograph for the 6 vol % hybrid silica added composite, it is evident that the filler particles are well-dispersed in the polymer matrix without any agglomeration. It is well-established that the polymer matrix interface and the dispersion of filler in the matrix play a major role in determining the overall properties of the composites including the mechanical properties.[26]

Figure 3 depicts the WAXD patterns of POSS, sPS, and their composites crystallized nonisothermally after melting at 280 °C under strictly controlled conditions. Before discussing the polymorphism of the sPS and its composites, it is worth mentioning that sPS exhibits five different crystalline forms (which are α, β, γ, δ, and ε) along with some other intermediate forms. Among these, the β form is the thermodynamically stable form that is resistant to the influence of solvents, and it will not undergo any transition before melting. It is interesting to note that the reflections at 2θ = 6.8, 10.3, 11.6, 13.4, 14.0, 15.5, 17.8, and 20.1° are signatures of the pristine sPS, which corresponds to the α form. On the other hand, in the case of sPS−hybrid silica composites, a few additional diffraction peaks were observed at 2θ = 6.2, 12.3, 18.6, and 21.3°, which are related to the thermodynamically stable β form.[18,27] It is evident from the WAXD analysis that the amount of the β form is monotonically increasing with the addition of the filler (Table

DOI: 10.1021/acsami.5b05933
ACS Appl. Mater. Interfaces 2015, 7, 19474−19483

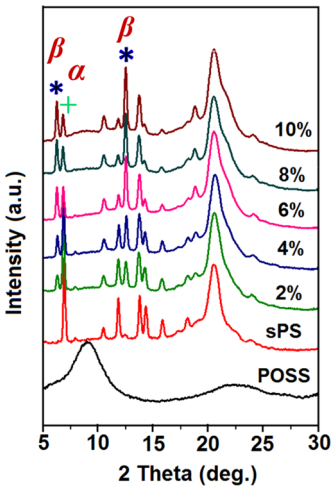

Figure 3. WAXD patterns of sPS and sPS/HS composites. SPS and its composites were crystallized nonisothermally after melting at 280 °C under tightly controlled conditions. The symbols: ∗ corresponds to the β form, and + corresponds to the α form of sPS.

1). The amount of β phase is estimated by dividing the area under the β reflections with the total area of α and β reflections.

Table 1. Percentage of β Phase Formation with Increase in Filler Loading and Avrami Constant (n) Values

Samples	Amount of β-phase (in %)	Avrami constant (n)
sPS	0	3
2% HS	26.2	2.4
4% HS	38.7	2.8
6% HS	50.0	2.9
8% HS	62.5	2.6
10% HS	78.6	2.3

In other words, it is obvious that the presence of hybrid silica spheres of POSS siloxane composition acts as the nucleating agent, which induces the β form of sPS with all-*trans*-planar-zigzag [T_4] chain conformation.[28] Formation of the thermodynamically stable β form in the end product is important since it can be used for wide variety of applications.

Besides microscopy, we have employed wide-angle X-ray diffraction (WAXD) also as an identification tool for the dispersibility of the filler in the polymer matrix. Evidently, no reflections corresponding to the filler are seen in the case of composites up to 6 vol % HS, which indicates the complete dispersion of hybrid silica in the sPS matrix. However, above 6 vol %, a weak reflection peak around $2\theta = 8°$ is observed, which arises due to the agglomeration of hybrid silica with POSS siloxane composition in the matrix.

The influence of hybrid silica spheres on the crystallization kinetics of sPS was studied with the help of differential scanning calorimetry (DSC). Figure 4a shows the DSC crystallization exotherms of pure sPS and its composites of varying compositions obtained at a cooling rate of 10 °C/min. With the addition of the filler, the melt crystallization temperature (T_{mc}) was found to be shifted to higher temperature regions, and its corresponding temperatures are summarized in Table S1 (Supporting Information). This increase in T_{mc} is due to the increased crystallization rate that resulted from the heterogeneous nucleation in the presence of the HS filler. However, increasing the HS addition beyond a threshold limit can result in agglomeration caused by the overloading. This is confirmed from the DSC cooling thermogram performed for 10 vol % HS added polymer composite which behaves anomalously (see Figure 4a).

Figure 4b shows the DSC thermograms of pure sPS and its composites as a function of crystallization time, where the samples were crystallized isothermally at 250 °C. The crystallization was performed under meticulous conditions, and the thermal program used for the crystallization of various samples is given in the Supporting Information (Figure S1). The crystallization half-time values measured at 250 °C for various samples are depicted in the Supporting Information (Table S1). These results can be explained by the fact that hybrid silica spheres act as heterogeneous nucleating agents, which have accelerated the crystallization rate of sPS. The relative crystallinity (X_t) at a given crystallization time was calculated from the DSC exotherms as described in the literature (obtained during the isothermal crystallization at 250 °C), and the plots of X_t against crystallization time for various samples are shown in Figure 5a. Relative crystallinity curves exhibit a sigmoid dependence on time.[29]

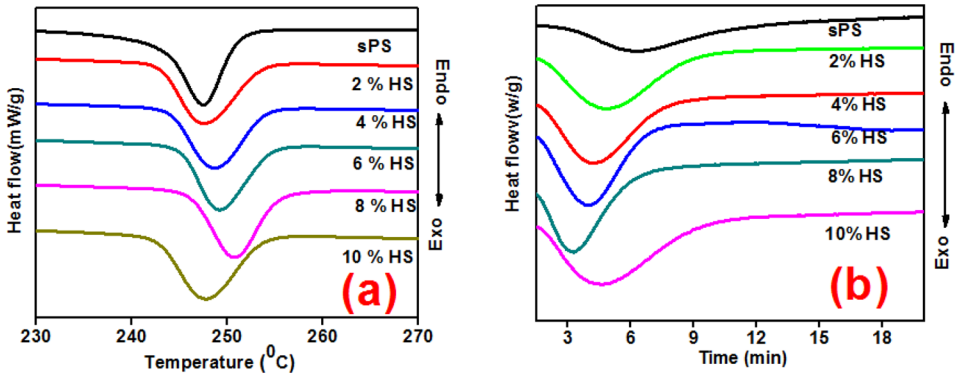

Figure 4. (a) DSC cooling thermograms of pure sPS and its composites crystallized nonisothermally after melting at 300 °C for 1 min. (b) DSC thermograms of isothermal crystallization at 250 °C/min for pure sPS and its composites.

DOI: 10.1021/acsami.5b05933
ACS Appl. Mater. Interfaces 2015, 7, 19474−19483

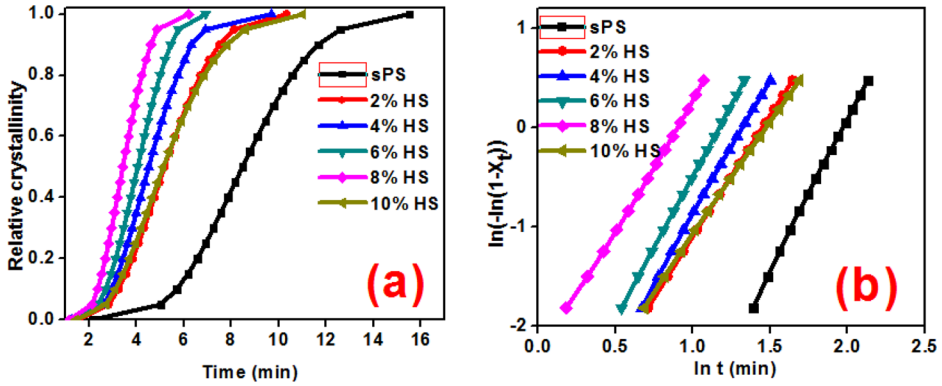

Figure 5. (a) Variation in relative crystallinity with crystallization time for pure sPS and its composites crystallized isothermally at 250 °C. (b) Plots of $\ln[-\ln(1 - X_t)]$ versus $\ln(t)$ for pure sPS and its composites crystallized isothermally at 250 °C.

In order to further elucidate the isothermal crystallization kinetics of pure sPS and its composites, an analysis based on the Avrami equation was carried out, which correlates the relative crystallinity (X_t) and crystallization time (t) according to

$$1 - X(t) = \exp(-Kt)^n \quad (1)$$

where n is the Avrami exponent that is dependent on the nature of nucleation and crystal growth geometry, and K is the overall isothermal crystallization rate constant (which is connected with both nucleation and crystal growth contributions).[30,31] The linear form of eq 1 can be written as

$$\ln[-\ln(1 - X_t)] = \ln K + n \ln(t) \quad (2)$$

By plotting $\ln[-\ln(1 - X_t)]$ versus $\ln(t)$, the Avrami parameters (n and K) were directly obtained from the slope and the intercept, respectively, from the early linear segment. Figure 5b represents plots for pure sPS and its composites along with the Avrami constants estimated for various samples crystallized at 250 °C. The n value of pure sPS was ~3.0, which was well comparable to the literature values.[32,33] This value of n indicates that pure sPS was crystallized by diffusion controlled spherulite growth (three-dimensional (3D) crystal growth) as a consequence of thermal nucleation. The Avrami constant computed for various sPS−HS compositions derived from Figure 5b is tabulated in Table 1. Interestingly, for composites, the calculated values of n assume values below 3, implying that the spherulite growth in these composites can be viewed as a combined effect of two-dimensional (2D) and three-dimensional (3D) growth mechanisms induced by the heterogeneous nucleation in the presence of HS as nucleating agent.

The thermogravimetric analysis (TGA) reveals a significant enhancement in the thermal stability of the composites compared to that of the pure polymer. The TGA plots given in Figure 6 clearly testify that their respective decomposition temperatures have been progressively increased as a function of HS content in the composites. When viewed at the 50% mass loss temperature, one can notice an enhancement by at least 30 °C in the decomposition temperature of sPS with HS additive compared to that of pure sPS. The 10% weight loss temperature ($T_{0.1}$) and 50% weight loss temperature ($T_{0.5}$) are summarized in Table 2. The residual weight observed in the TGA curves can be attributed to the hybrid silica content in the composites. Here, the well-dispersed hybrid silica fillers with the POSS siloxane composition which are having high heat

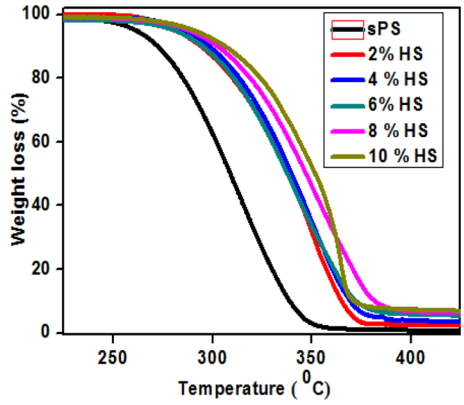

Figure 6. TGA thermograms for sPS and its composites from 0 to 10 vol % of hybrid silica content.

Table 2. 10% Weight Loss Temperature ($T_{0.5}$) and 50% Weight Loss Temperature ($T_{0.1}$)

Sample	10% weight loss temperature (°C) (±1)	50% weight loss temperature (°C) (±1)
sPS	272	308
2% HS	294	338
4% HS	298	340
6% HS	294	338
8% HS	302	348
10% HS	306	352

resistant property will delay the decomposition temperature of composites.[34,35]

Low coefficient of thermal expansion is an important factor in the case of ILDs in microelectronic devices, where materials with near the CTE of copper (17 ppm/°C)[36] are beneficial for reliability. Thermomechanical analysis was carried out to investigate the thermal expansion behavior of the pure polymer as well as sPS−6 vol % HS added composites. The coefficient of thermal expansion is found to be decreased considerably

DOI: 10.1021/acsami.5b05933
ACS Appl. Mater. Interfaces 2015, 7, 19474−19483

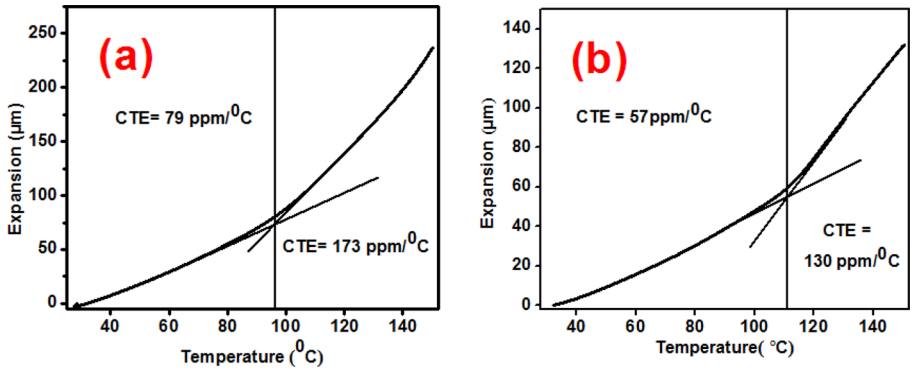

Figure 7. TMA analysis of (a) sPS and (b) sPS 6% filler loaded composites where the tangents are drawn to find the glass transition temperature.

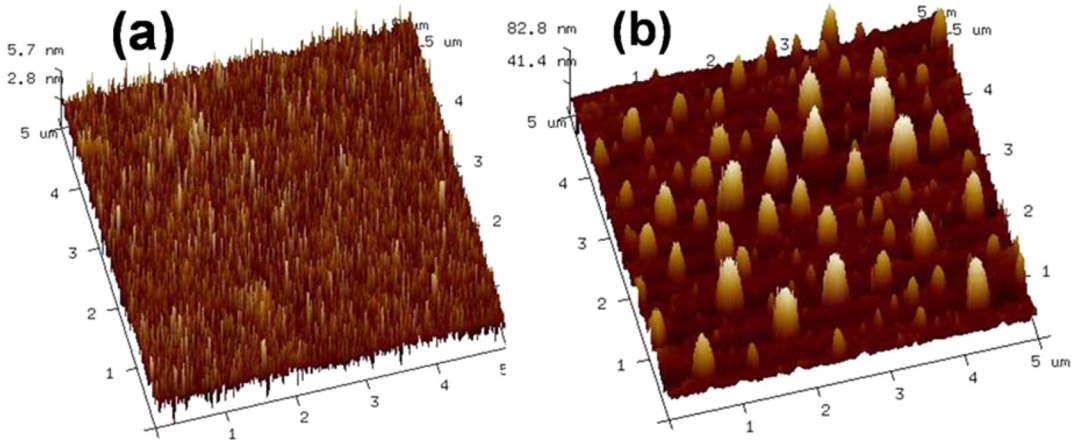

Figure 8. AFM images of (a) neat sPS film and (b) sPS/POSS composite film.

from 79 and 173 ppm/°C (before and after glass transition temperature) for sPS to 57 and 130 ppm/°C respectively, in the case of the composites (Figure 7a,b). There can be several reasons for this observation. Primarily, the inorganic Si−O−Si core of hybrid silica, which has an intrinsically low thermal expansion coefficient, might account for the decrease in CTE value of composites.[37] Pure silica has a CTE value of around 0.55 ppm/°C.[38,39] Second, the smaller HS particles with larger surface area interact more effectively with the sPS matrix, which can also reduce the thermal expansion of the composite. The glass transition temperature (T_g) of pure sPS is reported to be 97 °C, which is confirmed in the present investigation also. The variation of CTE before and after T_g is very clear from the graphs. This is due to the enhanced segmental mobility of the polymer chains after T_g. The T_g of the composite is found to be increased by 14 °C in the case of sPS−6 vol % HS composites, which is estimated from the tangent of the two slopes in the curve. The increase in the T_g is due to the hindrance of the mobility of polymer segments, which can be attributed to the effective interfacial interaction between the polymer chains and the hybrid silica fillers.

Film uniformity and surface roughness of the material play a vital role in the fabrication stages of an ILD. This is because, while fabricating interconnects of copper with porous ultralow-κ interlayer dielectrics, the high diffusivity of copper drives them into the pores of low-κ materials, which can result in serious device degradation and failure. To check the surface smoothness of the composite surfaces, we have performed AFM studies that revealed that the surface roughness is within the acceptable limits of what the industry needs. The surface roughness is 15 and 26 nm, respectively, for neat polymer and for the composites, respectively. Another important parameter is surface skewness (R_{sk}), which is a measure of the average of the first derivative of the surface (the departure of the surface from symmetry). A negative value of R_{sk} indicates that the surface is made up of valleys, whereas a surface with a positive skewness is said to contain mainly peaks and asperities.[24,25] In the present investigation, the R_{sk} value for a typical sPS−6 vol % HS composite is found to be −0.0928. The homogeneous dispersion of the HS filler in the polymer matrix is also clearly evidenced from the AFM analysis (see Figure 8b).

As documented well in the literature, implementation of low-κ dielectric material is one of several strategies used to allow continued scaling of microelectronic devices, extending Moore's law. With several decades of continuing miniaturization, the insulating dielectrics have thinned to the point where charge builds up and crosstalk adversely affects the performance of the device. Replacing the silicon dioxide with a low-κ dielectric of the same thickness can effectively reduce parasitic capacitance, enabling faster switching speeds and lower heat dissipation.[40] With this objective, the dielectric characteristic of the newly developed low-κ compositions were studied both in the RF and microwave regions. It is well-known that the relative permittivity or dielectric constant of a material is a frequency-dependent phenomenon and is a resultant of four different polarization mechanisms, which are space charge polarization, dipolar polarization, ionic polarization, and electronic polarization.[41] Syndiotactic polystyrene, being a nonpolar polymer, is likely to possess a low dielectric constant due to its peculiar conformation of the phenyl groups

DOI: 10.1021/acsami.5b05933
ACS Appl. Mater. Interfaces 2015, 7, 19474−19483

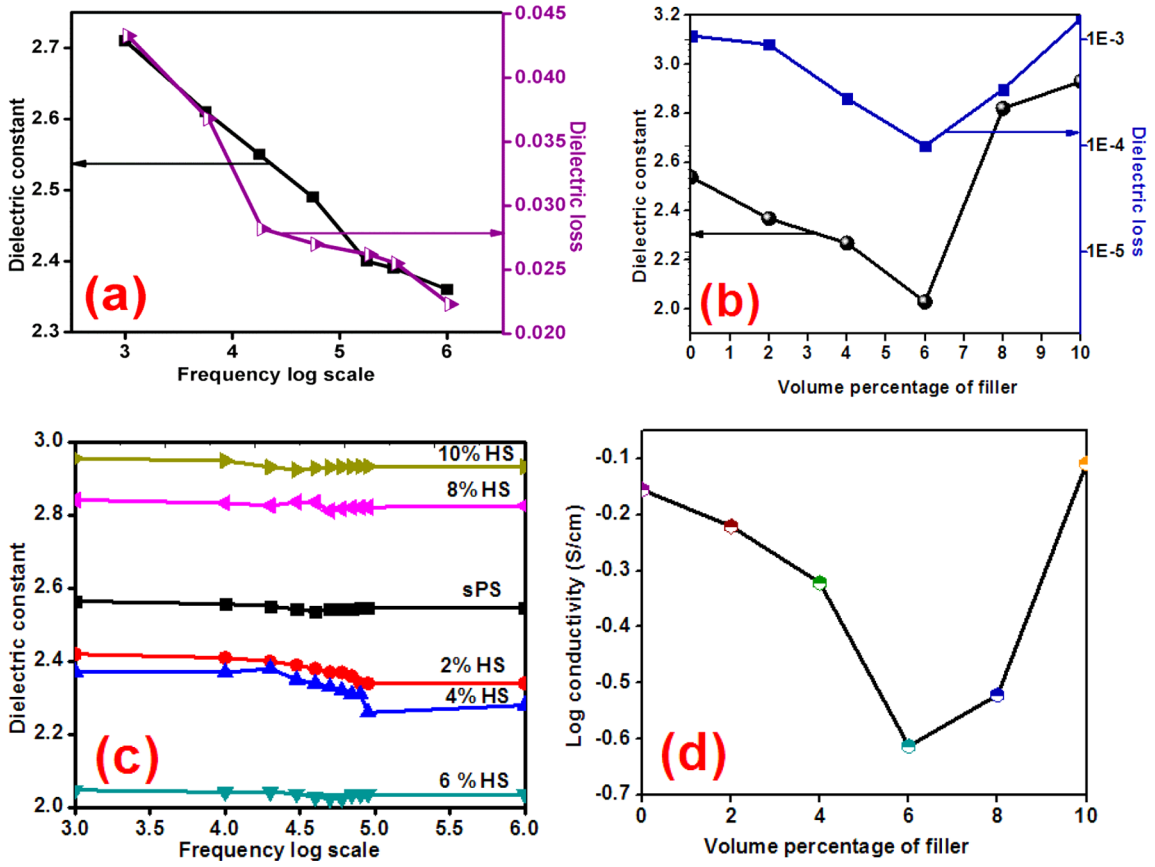

Figure 9. (a) Variation of dielectric constant and dielectric loss of hybrid silica spheres of POSS siloxane composition with respect to frequency. (b) Variation of dielectric constant and dielectric loss of sPS and its composites with different percent filler loading at 1 MHz. (c) Variation of dielectric constant of sPS and its composites with different percent filler loading with respect to frequency. (d) Variation of log conductivity of sPS and its composites with different percent filler loading at 1 MHz.

positioned on alternating sides of the hydrocarbon backbone. In heterogeneous systems such as sPS−POSS composites, space charge can be developed at the electrode−dielectric interface or in the amorphous and crystalline regions of the semicrystalline polymer. The contribution to space charge polarization could be restricted to the lower end of radio frequency while dipolar polarization could even extend up to microwave frequencies, above which ionic polarization takes over. Hence, in the present investigation, either dipolar, ionic, or a combination of both of these polarizations could be contributing to the dielectric constant values of the composites measured at microwave frequency (5 GHz).

Figure 9a shows the dependence of dielectric constant (κ) and dielectric loss (tan δ) of hybrid silica as a function of RF frequency. As explained before, the hybrid silica used in the present investigation is amphiphilic in nature, due to the presence of hydrophilic amino groups, which will help in the self-catalysis[22] of the HS formation and hydrophobic vinyl groups. The vinyl groups will promote the effective interaction of HS with the polymer matrix and will drive away the water molecules, whereby lowering the sensitivities to moisture. The apparent dielectric constant of HS is 2.36 (at 1 MHz), and the dielectric loss is 2.2×10^{-2}. It is found that the dielectric constant of HS can be effectively tuned by varying the organic chain length. However, the exact mechanism correlating the dielectric constant to their molecular structures, so far, has not been fully understood. The observation of a low κ value for hybrid silica is a clear indicator that its hydrophobic functionalization using vinyl groups is effective in controlling its sensitivity to moisture. The low dielectric constant of HS is largely dependent on its nanoporosity of the cube cage structure since porosity will always lead to lower dielectric constants owing to the lowest dielectric constant value of air (κ = 1).[42]

Syndiotactic polystyrene has a lower dielectric constant than atactic polystyrene (κ = 3.2).[16,43] This is due to the spatial arrangement of the phenyl side groups on the polymer backbone, which results in a net decreased dipole moment, eventually leading to a lower dielectric constant. The variation in the dielectric constant and dielectric loss of sPS−hybrid silica composites of various compositions with respect to the fillers are shown in Figure 9b. The dielectric constant and dielectric loss decrease up to 6 vol % and then increase. This increase can be due to the agglomeration of HS in the polymer matrix after the optimum loading, where the organic functional groups present on the HS enhance the possibility of polarization and moisture absorption. The dielectric constant of the pristine polymer is 2.53 at 1 MHz, which decreases to 2.03 with the addition of 6 vol % filler and then increases on further addition of filler. The decreased value of dielectric constant for the sPS−6 vol % HS composite can be explained using three possible reasons. In the present case, the host matrix in the composites existed as a mixture of α and β forms having a planar zigzag conformation with the aromatic groups on the opposite sides. This syndiotactic arrangement with reduced dipole moment is believed to be the primary reason behind the reduced relative

DOI: 10.1021/acsami.5b05933
ACS Appl. Mater. Interfaces 2015, 7, 19474−19483

permittivity. Second, the intrinsic dielectric constant of the hydrophobic POSS moiety is low, which can definitely help to reduce the dielectric constant.[15,44] Another reason can be a common feature seen in several polymer−ceramic composites, where a reduction in the net polarization of the polymer matrix is expected due to the hindrance caused by the filler that are well-intercalated and dispersed in the polymer matrix. This argument can be further validated by the observation of an increase in T_g in sPS−HS composites, as observed from the TMA analysis (see Figure 7a,b), which indirectly hints at the hindrance in the segmental mobility of the polymer matrix. From the preceding discussion, it is clearly understood that there will be the formation of an immobilized region of polymer chains around the hybrid silica fillers, which will decrease the overall polarization, eventually leading to a decreased dielectric constant. Variation of relative permittivity for different compositions as a function of RF frequency is given in Figure 9c. The dielectric loss of the 6 vol % composition is also found to be very interesting with the lowest measured value of loss, in the range of 10^{-4}. The low dielectric loss of the composites can be attributed to the low electrical conductivity observed in the case of composites, which is shown in Figure 9d. It is worthwhile to note that the ac conductivity of the composition of 6% HS shows the lowest value of electrical conductivity, which is an indicator of lower charge carrier density at this filler addition. The increase in the loss tangent after 6 vol % filler loading can be ascribed to the increased moisture absorption and agglomeration of the filler, which will enhance the polarization. The lowest possible concentration of dipoles and charge carriers with the lowest possible mobility will always lead to low loss in materials.[41]

In order to understand the microwave dielectric properties of the material, a split post dielectric resonator (SPDR) has been used where the quality factor and the resonant frequencies of SPDR before and after inserting the samples were measured from which the dielectric constant and loss were calculated.[45] The dielectric constant observed for 6 vol % HS added sPS composite at 5 GHz is 1.95, which is in well accordance with the theory that the dielectric constant value decreases with the increase in frequency as the polarization in the lower frequency region will not contribute at the higher frequency region. This is because the interfacial polarization can no longer follow rapid changes in the external electric field at microwave frequency where ionic polarization takes over.[46] The dielectric loss value obtained is 1×10^{-4}. This novel ultralow dielectric constant material made out of sPS−HS with POSS siloxane composition can be proposed as a next-generation ILD in the microelectronic devices.

The propensity of polymer composites to absorb water and cause a significant worsening of the dielectric properties is a very significant problem that can drastically deteriorate the dielectric, mechanical, and other properties of the composites.[5,47] The presence of highly polar water molecules will drastically increase the dielectric constant and dielectric loss of the composites (κ for water = 80).[3,48] Figure 10 shows that composites absorb moisture only negligibly and the percentage of absorption increases with the increase in filler loading. This increase can be attributed to the agglomeration of the filler particles and also due to the presence of the hydrophilic amino propyl group present in the POSS cage. In order to measure the moisture absorption, the weights of the samples were noted in dry condition, and, subsequently, the samples were dipped in distilled water for 24 h. They were then taken out, surface water

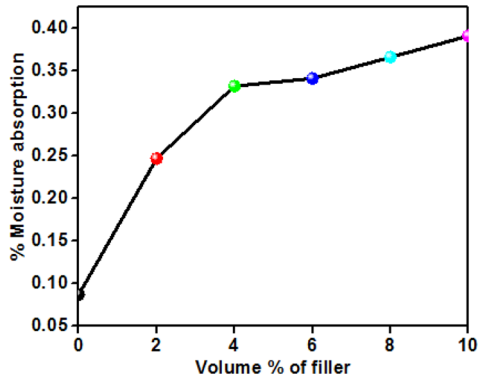

Figure 10. Variation of moisture absorption with respect to increase in the filler loading.

was wiped out, and they were weighed again. The percentage of water absorption can be calculated using the following equation, where W_i and W_f are weights of the samples before and after immersing in distilled water.

$$\%\ \text{moisture absorbed} = \frac{W_f - W_i}{W_i} \times 100$$

CONCLUSIONS

We successfully prepared a novel composite of thermally and chemically stable syndiotactic polystyrene with hybrid silica spheres of POSS siloxane composition which exhibited an ultralow dielectric constant of 1.95 with a very low loss of 1×10^{-4} at microwave frequency (5 GHz). The composites also exhibited enhanced microstructural homogeneity, better insensitivity toward moisture absorption, decreased thermal expansion coefficients, and effective surface roughness. In addition, it was found that the addition of the filler resulted in the formation of the thermodynamically stable β form of sPS, which extends its application. Also, the thermal stability of the composites was found to be increasing with the addition of the HS up to the percolation threshold. The excellent dielectrics, thermal and mechanical properties along with the stable β form make the material a promising candidate for a future-generation interlayer dielectric material.

ASSOCIATED CONTENT

Supporting Information

The Supporting Information is available free of charge on the ACS Publications website at DOI: 10.1021/acsami.5b05933.

Table S1: Melt crystallization temperatures and crystallization half times of neat sPS and its composites. Figure S1: Temperature program for isothermal crystallization of pure sPS and sPS/HS composites (PDF)

AUTHOR INFORMATION

Corresponding Authors

*E-mail: drkpsurendran@yahoo.com. Tel: +91-471-2515258. Fax: +91-471-2491712 (K.P.S.).

*E-mail: bhojegowd@niist.res.in. Tel: +91-471-2515474. Fax: +91-471-2491712 (E.B.G.).

Notes

The authors declare no competing financial interest.

DOI: 10.1021/acsami.5b05933
ACS Appl. Mater. Interfaces 2015, 7, 19474−19483

■ ACKNOWLEDGMENTS

The authors thank Dr. M. T. Sebastian for the constant encouragement and scientific discussions. The authors also thank Mr. M. R. Chandran, Dr. Yoosaf Karuvath, Mr. Aswin, and Mr. Kiran Mohan, CSIR - NIIST, for extending the SEM, AFM, and TEM facilities. A.M.J. thanks the University Grants Commission for the award of a research fellowship.

■ REFERENCES

(1) Kohl, P. A. Low−Dielectric Constant Insulators for Future Integrated Circuits and Packages. *Annu. Rev. Chem. Biomol. Eng.* **2011**, *2*, 379−401.
(2) de Theije, F. K.; Balkenende, A. R.; Verheijen, M. A.; Baklanov, M. R.; Mogilnikov, K. P.; Furukawa, Y. Structural Characterization of Mesoporous Organosilica Films for Ultralow-K Dielectrics. *J. Phys. Chem. B* **2003**, *107*, 4280−4289.
(3) Maex, K.; Baklanov, M. R.; Shamiryan, D.; lacopi, F.; Brongersma, S. H.; Yanovitskaya, Z. S. Low Dielectric Constant Materials for Microelectronics. *J. Appl. Phys.* **2003**, *93*, 8793−8841.
(4) Volksen, W.; Miller, R. D.; Dubois, G. Low Dielectric Constant Materials. *Chem. Rev.* **2010**, *110*, 56−110.
(5) Martin, S. J.; Godschalx, J. P.; Mills, M. E.; Shaffer, E. O., II; Townsend, P. H. Development of a Low-Dielectric-Constant Polymer for the Fabrication of Integrated Circuit Interconnect. *Adv. Mater.* **2000**, *12*, 1769−1778.
(6) Huang, X.; Zhi, C.; Jiang, P.; Golberg, D.; Bando, Y.; Tanaka, T. Polyhedral Oligosilsesquioxane-Modified Boron Nitride Nanotube Based Epoxy Nanocomposites: An Ideal Dielectric Material with High Thermal Conductivity. *Adv. Funct. Mater.* **2013**, *23*, 1824−1831.
(7) Sebastian, M. T.; Jantunen, H. Polymer−Ceramic Composites of 0−3 Connectivity for Circuits in Electronics: A Review. *Int. J. Appl. Ceram. Technol.* **2010**, *7*, 415−434.
(8) Grill, A.; Gates, S. M.; Ryan, T. E.; Nguyen, S. V.; Priyadarshini, D. Progress in the Development and Understanding of Advanced Low K and Ultralow K Dielectrics for Very Large-Scale Integrated Interconnects—State of the Art. *Appl. Phys. Rev.* **2014**, *1*, 011306−011317.
(9) Jin, C.; Lin, S.; Wetzel, J. T. Evaluation of Ultra-Low-K Dielectric Materials for Advanced Interconnects. *J. Electron. Mater.* **2001**, *30*, 284−289.
(10) Zhao, X.-Y.; Liu, H.-J. Review of Polymer Materials with Low Dielectric Constant. *Polym. Int.* **2010**, *59*, 597−606.
(11) Wang, J.-Y.; Yang, S.-Y.; Huang, Y.-L.; Tien, H.-W.; Chin, W.-K.; Ma, C.-C. M. Preparation and Properties of Graphene Oxide/Polyimide Composite Films with Low Dielectric Constant and Ultrahigh Strength Via in Situ Polymerization. *J. Mater. Chem.* **2011**, *21*, 13569−13575.
(12) Liao, W.-H.; Yang, S.-Y.; Hsiao, S.-T.; Wang, Y.-S.; Li, S.-M.; Ma, C.-C. M.; Tien, H.-W.; Zeng, S.-J. Effect of Octa(Aminophenyl) Polyhedral Oligomeric Silsesquioxane Functionalized Graphene Oxide on the Mechanical and Dielectric Properties of Polyimide Composites. *ACS Appl. Mater. Interfaces* **2014**, *6*, 15802−15812.
(13) Geng, Z.; Huo, M.; Mu, J.; Zhang, S.; Lu, Y.; Luan, J.; Huo, P.; Du, Y.; Wang, G. Ultra Low Dielectric Constant Soluble Polyhedral Oligomeric Silsesquioxane (Poss)−Poly(Aryl Ether Ketone) Nanocomposites with Excellent Thermal and Mechanical Properties. *J. Mater. Chem. C* **2014**, *2*, 1094−1103.
(14) Wu, J.; Mather, P. T. Poss Polymers: Physical Properties and Biomaterials Applications. *Polym. Rev.* **2009**, *49*, 25−63.
(15) Kuo, S.-W.; Chang, F.-C. Poss Related Polymer Nanocomposites. *Prog. Polym. Sci.* **2011**, *36*, 1649−1696.
(16) Sasikala, T. S.; Nair, B. P.; Pavithran, C.; Sebastian, M. T. Improved Dielectric and Mechanical Properties of Polystyrene−Hybrid Silica Sphere Composite Induced through Bifunctionalization at the Interface. *Langmuir* **2012**, *28*, 9742−9747.
(17) Hikosaka, S.; Ohki, Y. Effect of Tacticity on the Dielectric Properties of Polystyrene. *IEEJ Trans. Electr. Electron. Eng.* **2011**, *6*, 299−303.
(18) Gowd, E. B.; Tashiro, K.; Ramesh, C. Structural Phase Transitions of Syndiotactic Polystyrene. *Prog. Polym. Sci.* **2009**, *34*, 280−315.
(19) Jaymand, M. Recent Progress in the Chemical Modification of Syndiotactic Polystyrene. *Polym. Chem.* **2014**, *5*, 2663−2690.
(20) Gowd, E. B.; Shibayama, N.; Tashiro, K. Structural Correlation between Crystal Lattice and Lamellar Morphology in the Phase Transitions of Uniaxially Oriented Syndiotactic Polystyrene (δ and δ_e Forms) as Revealed by Simultaneous Measurements of Wide-Angle and Small-Angle X-Ray Scatterings. *Macromolecules* **2008**, *41*, 2541−2547.
(21) Shaiju, P.; Bhoje Gowd, E. Factors Controlling the Structure of Syndiotactic Polystyrene Upon the Guest Exchange and Guest Extraction Processes. *Polymer* **2015**, *56*, 581−589.
(22) Nair, B. P.; Pavithran, C. Bifunctionalized Hybrid Silica Spheres by Hydrolytic Cocondensation of 3-Aminopropyltriethoxysilane and Vinyltriethoxysilane. *Langmuir* **2010**, *26*, 730−735.
(23) Gupta, R.; Kandasubramanian, B. Hybrid Caged Nanostructure Ablative Composites of Octaphenyl-Poss/Rf as Heat Shields. *RSC Adv.* **2015**, *5*, 8757−8769.
(24) Tamaki, R.; Choi, J.; Laine, R. M. A Polyimide Nanocomposite from Octa(Aminophenyl)Silsesquioxane. *Chem. Mater.* **2003**, *15*, 793−797.
(25) Liang, K.; Li, G.; Toghiani, H.; Koo, J. H.; Pittman, C. U. Cyanate Ester/Polyhedral Oligomeric Silsesquioxane (Poss) Nanocomposites: Synthesis and Characterization. *Chem. Mater.* **2006**, *18*, 301−312.
(26) Hussain, F.; Hojjati, M.; Okamoto, M.; Gorga, R. E. Review Article: Polymer-Matrix Nanocomposites, Processing, Manufacturing, and Application: An Overview. *J. Compos. Mater.* **2006**, *40*, 1511−1575.
(27) Milano, G.; Guerra, G. Understanding at Molecular Level of Nanoporous and Co-Crystalline Materials Based on Syndiotactic Polystyrene. *Prog. Mater. Sci.* **2009**, *54*, 68−88.
(28) Chatani, Y.; Shimane, Y.; Ijitsu, T.; Yukinari, T. Structural Study on Syndiotactic Polystyrene: 3. Crystal Structure of Planar Form I. *Polymer* **1993**, *34*, 1625−1629.
(29) Nagendra, B.; Mohan, K.; Bhoje Gowd, E. Polypropylene/Layered Double Hydroxide (LDH) Nanocomposites: Influence of LDHs Particle Size on the Crystallization Behavior of Polypropylene. *ACS Appl. Mater. Interfaces* **2015**, *7*, 12399−12410.
(30) Avrami, M. Kinetics of Phase Change. I General Theory. *J. Chem. Phys.* **1939**, *7*, 1103−1112.
(31) Avrami, M. Kinetics of Phase Change. Ii Transformation-Time Relations for Random Distribution of Nuclei. *J. Chem. Phys.* **1940**, *8*, 212−224.
(32) Tseng, C.-R.; Lee, H.-Y.; Chang, F.-C. Crystallization Kinetics and Crystallization Behavior of Syndiotactic Polystyrene/Clay Nanocomposites. *J. Polym. Sci., Part B: Polym. Phys.* **2001**, *39*, 2097−2107.
(33) Papageorgiou, G. Z.; Achilias, D. S.; Nianias, N. P.; Trikalitis, P.; Bikiaris, D. N. Effect of the Type of Nano-Filler on the Crystallization and Mechanical Properties of Syndiotactic Polystyrene Based Nanocomposites. *Thermochim. Acta* **2013**, *565*, 82−94.
(34) Chruściel, J. J.; Leśniak, E. Modification of Epoxy Resins with Functional Silanes, Polysiloxanes, Silsesquioxanes, Silica and Silicates. *Prog. Polym. Sci.* **2015**, *41*, 67−121.
(35) Choi, J.; Tamaki, R.; Kim, S. G.; Laine, R. M. Organic/Inorganic Imide Nanocomposites from Aminophenylsilsesquioxanes. *Chem. Mater.* **2003**, *15*, 3365−3375.
(36) Jin, S.; Mavoori, H. Low-Thermal-Expansion Copper Composites Via Negative Cte Metallic Elements. *JOM* **1998**, *50*, 70−72.
(37) Sulaiman, S.; Brick, C. M.; De Sana, C. M.; Katzenstein, J. M.; Laine, R. M.; Basheer, R. A. Tailoring the Global Properties of Nanocomposites. Epoxy Resins with Very Low Coefficients of Thermal Expansion. *Macromolecules* **2006**, *39*, 5167−5169.
(38) Tada, H.; Kumpel, A. E.; Lathrop, R. E.; Slanina, J. B.; Nieva, P.; Zavracky, P.; Miaoulis, I. N.; Wong, P. Y. Thermal Expansion

DOI: 10.1021/acsami.5b05933
ACS Appl. Mater. Interfaces 2015, 7, 19474−19483

Coefficient of Polycrystalline Silicon and Silicon Dioxide Thin Films at High Temperatures. *J. Appl. Phys.* **2000**, *87*, 4189−4193.
(39) Zhao, J.-H.; Ryan, T.; Ho, P. S.; McKerrow, A. J.; Shih, W.-Y. Measurement of Elastic Modulus, Poisson Ratio, and Coefficient of Thermal Expansion of on-Wafer Submicron Films. *J. Appl. Phys.* **1999**, *85*, 6421−6424.
(40) Maier, G. Low Dielectric Constant Polymers for Microelectronics. *Prog. Polym. Sci.* **2001**, *26*, 3−65.
(41) Sebastian, M. T. Measurement of Microwave Dielectric Properties and Factors Affecting Them. In *Dielectric Materials for Wireless Communication*; Sebastian, M. T., Ed.; Elsevier: Amsterdam, 2008; Chapter 2, pp 11−47.
(42) Leu, C.-M.; Chang, Y.-T.; Wei, K.-H. Polyimide-Side-Chain Tethered Polyhedral Oligomeric Silsesquioxane Nanocomposites for Low-Dielectric Film Applications. *Chem. Mater.* **2003**, *15*, 3721−3727.
(43) He, F.; Lam, K.-H.; Fan, J.; Chan, L. H. Improved Dielectric Properties for Chemically Functionalized Exfoliated Graphite Nanoplates/Syndiotactic Polystyrene Composites Prepared by a Solution-Blending Method. *Carbon* **2014**, *80*, 496−503.
(44) Zhang, C.; Guang, S.; Zhu, X.; Xu, H.; Liu, X.; Jiang, M. Mechanism of Dielectric Constant Variation of Poss-Based Organic−Inorganic Molecular Hybrids. *J. Phys. Chem. C* **2010**, *114*, 22455−22461.
(45) Krupka, J. Frequency Domain Complex Permittivity Measurements at Microwave Frequencies. *Meas. Sci. Technol.* **2006**, *17*, R55−R70.
(46) Kim, J.-Y.; Lee, W. H.; Suk, J. W.; Potts, J. R.; Chou, H.; Kholmanov, I. N.; Piner, R. D.; Lee, J.; Akinwande, D.; Ruoff, R. S. Chlorination of Reduced Graphene Oxide Enhances the Dielectric Constant of Reduced Graphene Oxide/Polymer Composites. *Adv. Mater.* **2013**, *25*, 2308−2313.
(47) Yuan, C.; Wang, J.; Jin, K.; Diao, S.; Sun, J.; Tong, J.; Fang, Q. Postpolymerization of Functional Organosiloxanes: An Efficient Strategy for Preparation of Low-Kmaterial with Enhanced Thermostability and Mechanical Properties. *Macromolecules* **2014**, *47*, 6311−6315.
(48) Kohmura, K.; Tanaka, H.; Oike, S.; Murakami, M.; Fujii, N.; Takada, S.; Ono, T.; Seino, Y.; Kikkawa, T. Novel Organosiloxane Vapor Annealing Process for Improving Properties of Porous Low-K Films. *Thin Solid Films* **2007**, *515*, 5019−5024.

DOI: 10.1021/acsami.5b05933
ACS Appl. Mater. Interfaces 2015, 7, 19474−19483